analytical chemistry

Article

pubs.acs.org/ac

Phospholipid–Graphene Nanoassembly as a Fluorescence Biosensor for Sensitive Detection of Phospholipase D Activity

Si-Jia Liu, Qian Wen, Li-Juan Tang,* and Jian-Hui Jiang*

State Key Laboratory of Chemo/Bio-Sensing and Chemometrics, College of Chemistry and Chemical Engineering, Hunan University, Changsha, 410082, People's Republic of China

Supporting Information

ABSTRACT: A novel phospholipid–graphene nanoassembly is developed based on self-assembly of phospholipids on nonoxidative graphene surfaces. The nanoassembly can be prepared easily through noncovalent hydrophobic interactions between the lipid tails and the graphene without destroying the electronic conjugation within the graphene sheet. This imparts the nanoassembly with desired electrical and optical properties with nonoxidative graphene. The phospholipid coating offers excellent biocompatibility, facile solubilization, and controlled surface modification for graphene, making the nanoassembly a useful platform for biofunctionalization of graphene. The nanoassembly is revealed to comprise a bilayer of phospholipids with a reduced graphene oxide sheet hosting in the hydrophobic interior, thus affording a unique planar mimic of the cellular membrane. By using a fluorescein-labeled phospholipid in this nanoassembly, a fluorescence biosensor is developed for activity assay of phospholipase D. The developed biosensor is demonstrated to have high sensitivity, wide dynamic range, and very low detection limit of 0.010 U/L. Moreover, because of its single-step homogeneous assay format it displays excellent robustness, improved assay simplicity and throughput, as well as intrinsic ability to real-time monitor the reaction kinetics.

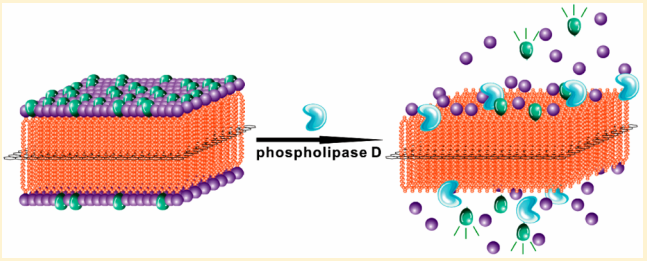

Graphene, a one-atom layer, two-dimensional structured graphite with excellent mechanical, thermal, electrical, and optical properties, creates a unique component in constructing tailor-made composite materials for biological applications.[1,2] The key step toward these materials is the solubilization and biofunctionalization of graphene. There has been significant progress in the development of various covalent and noncovalent functionalization methods for biological modification and solubilization of graphene.[3−12] Among these, most works rely on the use of oxidative chemistry, and the resulting graphene oxide can comprise abundant reactive and hydrophilic functional groups including carboxylic acid, hydroxyl, epoxide, and carbonyl, which renders this material highly soluble and versatile for covalent conjugation of biomolecules.[3−5] Alternatively, the soluble graphene oxide possesses a basal aromatic plane allowing strong $\pi-\pi$ stacking interactions with aromatic molecules. This constitutes a useful platform for noncovalent assembly of biological components such as DNA and peptides.[6−10] However, very few studies have been performed on the implementation of nonoxidative graphene for biological modification and solubilization,[11,12] which is contrasted with its cousin carbon nanotubes that are predominantly used in a nonoxidative state for biofunctionalization.[13−15] Because graphene in a nonoxidative state may offer substantially improved electrical and optical performance,[1,2,16] development of biofunctionalization methods for nonoxidative graphene may provide a new paradigm for further expanding the area of graphene-based biological applications.

Phospholipids, in addition to their function as the structural components of cell membranes, are major elements of complex intracellular signaling networks. Specifically, phospholipid signaling plays a crucial role in growth, metabolism, differentiation, apoptosis, membrane trafficking, and action cytoskeleton rearrangement.[17,18] In the context, phospholipid-functionalized nanomaterials represent an attractive option for the studies of phospholipid signaling. Hence, there have been widespread implementations of phospholipids for functionalization of various nanomaterials including carbon nanotubes,[14,15] gold nanoparticles,[19] silica nanoparticles, and so on.[20−23] These phospholipid-functionalized nanocomposites have demonstrated great potential for intracellular delivery of analytical probes or therapeutic drugs[19−22] and development of biotracers, biosensors, or bioelectronic devices.[15,23] Surprisingly, to date the biofunctionalization and solubilization of graphene with phospholipids have been largely unexplored.

Considering the hydrophobicity of graphene surface, herein we explore whether the phospholipids can be self-assembled on the graphene surface due to the hydrophobic interactions between the lipid tails and the graphene. This allows us to develop a novel phospholipid–graphene nanoassembly from phospholipid-based functionalization of nonoxidative graphene. Such a nanoassembly may be advantageous over graphene

Received: February 22, 2012
Accepted: June 20, 2012
Published: June 20, 2012

dx.doi.org/10.1021/ac300539s | *Anal. Chem.* 2012, 84, 5944–5950

oxide derivatives, because the phospholipid coating offers excellent biocompatibility, facile solubilization, and controlled surface modification for graphene without altering its electronic conjugation structure. To our knowledge, there is no report concerning the phospholipid-based solubilization of nonoxidative graphene for biological analysis applications except for some theoretical simulations of phospholipid−graphene interactions[24,25] and the development of graphene-based electronic surface with lipid modification.[26] Thus, the developed phospholipid−graphene nanoassembly may constitute an innovative platform for biofunctionalization and solubilization of nonoxidative graphene and for further expansion of graphene-based biological applications. As a case study, we demonstrate that this nanoassembly can be adapted into a novel fluorescence biosensor for activity assay of phospholipase D by using a fluorescein-labeled phospholipid for the functionalization. Phospholipase D is an enzyme catalyzing the hydrolysis of phosphatidylcholine into choline and phosphatidic acid, an established intracellular signaling lipid that is implicated in vesicular trafficking.[27] Activity assay of phospholipase D is thus of considerable importance for understanding and regulating many biological processes such as lipid metabolism, inflammation, cellular signaling, and cancer development.[28] Compared with existing methods for phospholipase D assay based on chromatography,[29] fluorescence resonance energy transfer,[30] mass spectrometry,[31] or electrochemistry,[32] the developed biosensor may afford better sensitivity and higher robustness as well as improved assay simplicity and throughput.

EXPERIMENTAL SECTION

Reagents and Materials. Graphite powder (99.95%, 325 mesh) was purchased from Alfa Aesar (Massachusetts, U.S.A.). Phospholipase D from *Streptomyces chromofuscus* (PLD) was obtained from Merck (Darmstadt, Germany). *N*-(Fluorescein-5-thiocarbamoyl)-1,2-dihexadecanoyl-*sn*-glycero-3-phosphoethanolamine (FL-DHPE) was purchased from Invitrogen (California, U.S.A.). Dipalmitoyl-*sn*-glycero-3-phosphocholine (DPPC), cholesterol, halopemide, ethylenediaminetetraacetic acid (EDTA), human serum albumin (HSA), and *N*,*N*-dimethylmethanamide (DMF) were from Sigma-Aldrich (Missouri, U.S.A.). All other chemicals were of analytical grade and obtained from Sinopharm Chemical Reagent Co. Ltd. (Shanghai, China). All solutions were prepared using ultrapure water, which was obtained through a Millipore Milli-Q water purification system (Billerica, MA, U.S.A.) and had an electric resistance >18.3 MΩ.

Preparation of the Phospholipid−Graphene Nanoassembly. Liposome was synthesized according to a documented protocol[33] with minor modifications. Briefly, DPPC, cholesterol, and FL-DHPE in 4:1:1 molar ratio (3.6 mg in total) were dissolved in 3 mL of chloroform in a round-bottom flask and dried in a rotary evaporator under reduced pressure at 30 °C to form a thin lipid film on the inside wall of the flask. The lipid film was hydrated with 4 mL of ultrapure water at 60 °C for 1 h followed by sonication for 1 h in ice−water bath by a probe-type sonicator using a power of 25 W. The resulting liposome suspension was centrifuged at 5000 rpm for 15 min to remove undispersed lipids and multilamellar vesicles. Graphene oxide was prepared by a modified Hummers method using graphite powder as starting material as described previously.[34] The graphene oxide was reduced with hydrazine at 100 °C for over 24 h to obtain the nonoxidative graphene or reduced graphene oxide (RGO). (Note: *Reduced graphene oxide was a chemically modified graphene rather than "pristine" graphene. Because our study only involved noncovalent modification of reduced graphene oxide by phospholipids, in which reduced graphene oxide showed very similar properties to graphene, the terminology "graphene" was used instead of reduced graphene oxide for simplicity.*) Prior to use, reduced graphene oxide suspension was obtained by dispersing 2 mg of as-prepared graphene powder in 4 mL of ultrapure water in an ice bath using the probe-type sonicator under a power of 25 W for 1 h. A 1 mL aliquot of the prepared liposome was mixed with 2 mL of RGO suspension followed by sonication for 2 h in ice−water bath by the probe-type sonicator using a power of 25 W. The resulting mixture was centrifuged at 5000 rpm for 15 min to remove large aggregates, and the supernate containing stable suspension of phospholipid−graphene nanoassembly was collected and diluted to 5 mL with ultrapure water. After the weighing of collected large aggregates of RGO, the phospholipid−graphene nanoassembly suspension was estimated to contain ∼0.3 mg/mL of RGO. Assuming no loss of FL-DHPE in the preparation of the nanoassembly, the concentration of FL-DHPE was estimated to ∼42 μM in the nanoassembly suspension. This nanoassembly suspension was stored at 4 °C for future use.

The as-prepared RGO and phospholipid−graphene nanoassembly were characterized using atomic force microscopy (AFM) and other procedures such as transmission electron microscope (TEM), Raman, infrared, and UV−vis spectroscopy, X-ray diffraction (XRD), X-ray photoelectron spectroscopy (XPS), and dynamic light scattering (DLS). The AFM images were taken using a Veeco Dimension V scanning probe microscope (Veeco Instruments Inc., U.S.A.). The sample films for AFM characterization were obtained by dropping the diluted solution of nanomaterial suspension on a freshly cleaved mica sheet and air-dried at room temperature. The resulting mica sheet was rinsed thoroughly with ultrapure water and dried in a nitrogen stream before the analysis.

Phospholipid−Graphene Nanoassembly-Based Assay of Phospholipase D Activity. The reaction solution was prepared in fresh by mixing 6 μL of phospholipid−graphene nanoassembly suspension with 14 μL of reaction buffer containing 4 μL of Tris−HCl buffer (50 mM, pH 8.0), 5 μL of 30% DMF, 1.5 μL of 100 mM $CaCl_2$, and 3.5 μL of ultrapure water. In a typical assay, in 20 μL of reaction solution, 10 μL of PLD (dissolved in 10 mM Tris−HCl buffer, pH 8.0 with final concentrations ranging from 0 to 1000 U/L) was added followed by incubation at 37 °C for 2 h. The resulting mixture was diluted to a final volume of 100 μL with ultrapure water and subjected to fluorescence measurements. The fluorescence spectra were recorded at room temperature in a 100 μL quartz cuvette on an F-7000 fluorescence spectrometer (Hitachi, Japan) equipped with a PMT (working voltage 950 V). The excitation wavelength was 492 nm, and the emission spectra were collected in the wavelength range from 505 to 600 nm with both excitation and emission slits of 2.5 nm.

The time-dependent fluorescence measurements was performed immediately on adding 40 μL of PLD (dissolved in 10 mM Tris−HCl, pH 8.0, final concentrations ranging from 0 to 1000 U/L) in 80 μL of reaction solution in the 100 μL quartz cuvette on the F-7000 spectrofluorometer. The excitation wavelength was set to 492 nm (slit 2.5 nm), and the emission wavelength was 514 nm (slit 2.5 nm) with a time interval of 8 s

dx.doi.org/10.1021/ac300539s | *Anal. Chem.* 2012, 84, 5944−5950

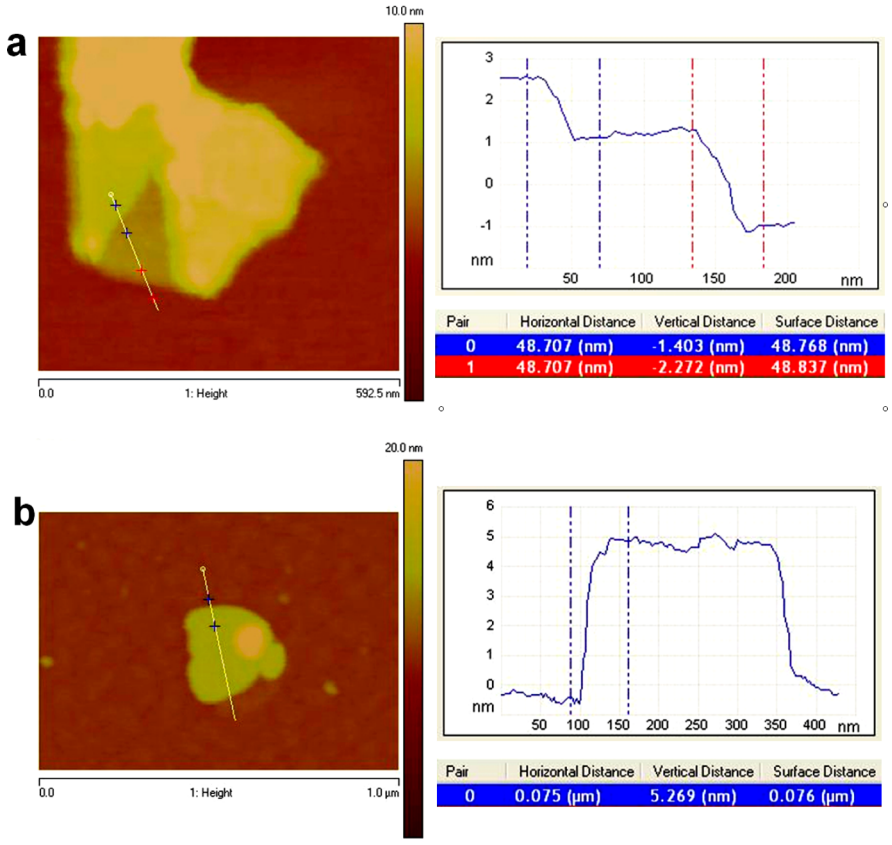

Figure 1. AFM images (left) and height profiles (right) of freshly prepared reduced graphene oxide (a) and as-prepared phospholipid–graphene nanoassembly (b).

at a controlled temperature of 25 °C under a PMT voltage of 700 V.

RESULTS AND DISCUSSION

Characterization of the Phospholipid–Graphene Nanoassembly. We explored the use of hydrophobic interactions between the lipid tails and the graphene to prepare the phospholipid–graphene nanoassembly. This nanoassembly could be obtained readily by mixing the liposome with graphene suspension under sonication. The as-prepared phospholipid–graphene nanoassembly was characterized using AFM to provide its morphological profile. After sonication treatment, the reduced graphene oxide sheets were well-dispersed on the mica surface, as shown in Figure 1. These graphene sheets gave a topological height of 1.4–2.3 nm, a typical vertical dimension for one- or two-layered sheets of graphene.[35,36] On the other hand, the phospholipid–graphene nanoassembly gave a topological height over 5.3 nm. According to the thickness of phospholipid bilayer (~4 nm),[33] the assembly of phospholipids was supposed to form a monolayer structure on either surfaces of reduced graphene oxide. Because of the hydrophobic effect energetically disfavoring the exposure of the hydrophobic lipid tails to aqueous surroundings and the hydrophobic forces between the lipid tails and graphene, this phospholipid monolayer would be arranged in such a structure: the hydrophilic phosphate heads pointed outward to aqueous surroundings on either side and the hydrophobic tails pointed inward to the graphene surface, as illustrated in Scheme 1. Additionally, the TEM images clearly illustrated that the reduced graphene oxide sheets and the phospholipid–graphene

Scheme 1. Structure of Assembled Monolayers of Phospholipids on Graphene Surfaces

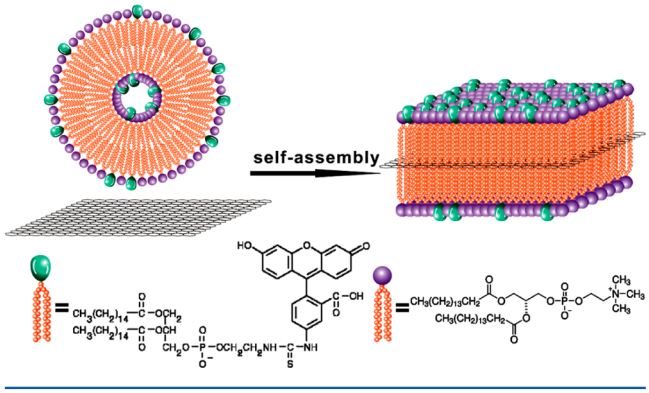

nanoassembly displayed a wrinkled structure and an ultrathin paperlike morphology (Figure S1 in the Supporting Information). Raman, infrared, and UV–vis spectroscopy, XRD, XPS, and DLS characterization also revealed that reduced graphene oxide showed much lower content of oxygen-containing functionalities and restored electronic conjugation within two-dimensional hexagonal platelet (Figures S2–S7 in the Supporting Information). Taken together, these data gave immediate evidence for successful preparation of the reduced graphene oxide sheets and the phospholipid–graphene nanoassembly.

Furthermore, it was observed that the reduced graphene oxide sheets agglomerated into large aggregates in aqueous solution and there were lots of sediments settled down at the

dx.doi.org/10.1021/ac300539s | Anal. Chem. 2012, 84, 5944–5950

bottom of the vial (Figure 2). By contrast, the phospholipid–graphene nanoassembly appeared to be very homogeneous and

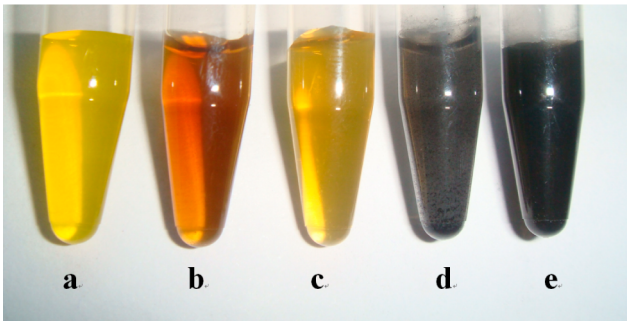

Figure 2. Photograph of suspensions for liposome (a), graphene oxide (b), phospholipid-coated graphene oxide (c), reduced graphene oxide (d), and phospholipid–graphene nanoassembly (e).

stable (no sediments observed for at least 2 months) in water. Such excellent solubility and stability in aqueous solution as well as the phospholipid-based biocompatible coating favorably supported the potential of the phospholipid–graphene nanoassembly for biological applications. For a comparison between the phospholipid–graphene nanoassembly and graphene oxide, we also prepared the phospholipid-coated graphene oxide using a procedure similar to that for the phospholipid–graphene nanoassembly. Interestingly, the phospholipid-coated graphene oxide suspensions were found to display a color clearly different from that of the phospholipid–graphene nanoassembly, with appreciable darkening observed for the phospholipid–graphene nanoassembly with reference to the counterpart of graphene oxide. This color change was attributed to the restoration of electronic conjugation within the nonoxidative graphene sheet during the reduction reaction. In other words, the phospholipid–graphene nanoassembly showed a much stronger absorption of energy ranging in the visible spectrum than its graphene oxide counterpart. This might be an advantage in applications where this nanoassembly was utilized as an efficient energy acceptor for biological analysis based on fluorescence resonant energy transfer.[16]

It is noteworthy that the developed phospholipid–graphene nanoassembly may have several advantages over existing solubilization methods for graphene such as graphene oxide and graphene–polymer composites.[37] First, the phospholipid–graphene nanoassembly could be prepared very easily through noncovalent assembly. This could retain electronic conjugation within the nonoxidative graphene sheet and thus ensure the desired electrical and optical properties intrinsical in graphene, whereas oxidation or covalent grafting would alter these electrical and optical properties because of the distortion of electronic conjugation structure. Second, the nanoassembly was highly soluble and stable in aqueous solution, and the phospholipid coating imparted the nanoassembly with excellent biocompatibility. This made the developed nanoassembly an ideal nanocomposite used in biological surroundings. Third, the composition of the monolayer phospholipid coating could be readily designed and controlled by using various commercially available phospholipid derivatives and even other lipid analogues. This allowed the displaying of various functional groups, signal reporters, and biological ligands at the outward surface of the phospholipid coating. In this setting, the developed nanoassembly might constitute a versatile platform for biofunctionalization of nonoxidative graphene and related biological applications. In the present study, we demonstrate a model application of this nanoassembly as a novel fluorescence biosensor for activity assay of phospholipase D by using a fluorescein-labeled phospholipid for the functionalization.

Principle of the Phospholipid–Graphene Nanoassembly-Based Biosensor for Phospholipase D. Because graphene is intrinsically a fluorescence quencher for many fluorophores in proximity to its surface, self-assembly of a fluorescein-labeled phospholipid into a monolayer on the graphene surface can dramatically quench the fluorescence of these fluorescein labels. Motivated by this hypothesis, we developed a biosensor based on enzyme-catalyzed release of the fluorescein labels away from the fluorescence-quenched graphene-based nanoassembly. Scheme 2 illustrates the analytical principle of the biosensor for activity assay of phospholipase D. A nanoassembly of phospholipid-coated graphene was prepared using the liposome of two phospholipid components, the major one DPPC and the minor one FL-

Scheme 2. Analytical Principle of the Biosensor for Activity Assay of Phospholipase D

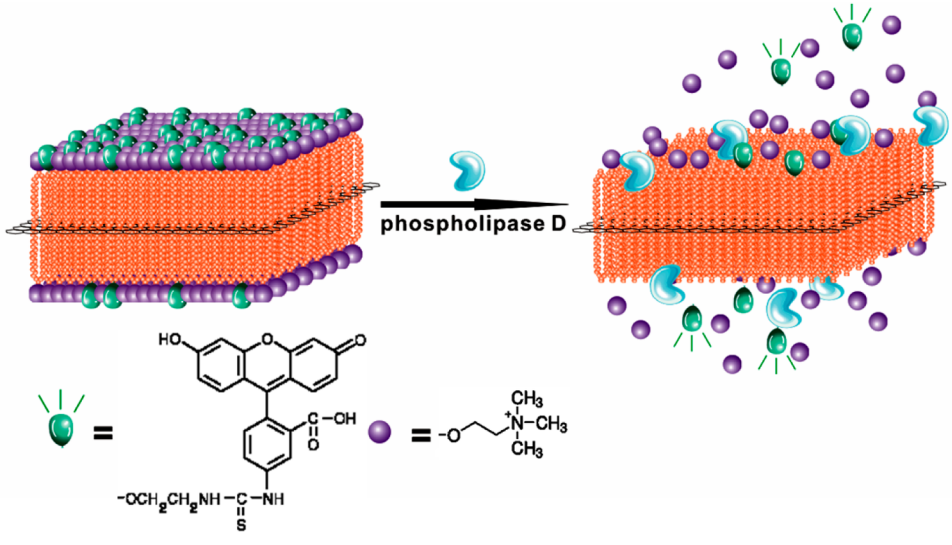

dx.doi.org/10.1021/ac300539s | Anal. Chem. 2012, 84, 5944–5950

DHPE, a derivative of 1,2-dihexadecanoyl-*sn*-glycero-3-phosphoethanolamine (DHPE) with a fluorescein label conjugated to the ethanolamine moiety. In this nanoassembly, the fluorescein labels were located in proximity to the graphene surface, and their fluorescence was quenched nearly completely due to efficient photoinduced energy or electron transfer processes. In the presence of active phospholipase D, the phosphodiester bonds after the phosphate were catalytically cleaved, which released the fluorescein labels apart from the graphene surface, thus activating their fluorescence signal. Because the cleavage of the fluorescein labels was highly selective to the enzymatic reaction, the resulting fluorescence response could then give an indicator for the activity of phospholipase D.

Figure 3 depicts typical fluorescence spectral responses of the biosensor in the assay of phospholipase D. The nanoassembly

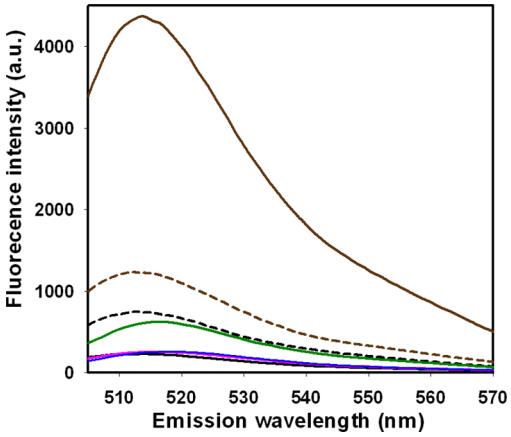

Figure 3. Fluorescence spectra obtained for phospholipid−graphene nanoassembly (black solid line), phospholipid-coated graphene oxide suspension (black dashed line), phospholipid−graphene nanoassembly plus 1000 U/L PLD (brown solid line), phospholipid-coated graphene oxide suspension plus 1000 U/L PLD (blown dashed line), phospholipid−graphene nanoassembly plus 5% HSA (blue solid line), phospholipid−graphene nanoassembly plus 1000 U/L PLD in the presence of 1 mg/mL inhibitor halopemide (green solid line), phospholipid−graphene nanoassembly plus 1000 U/L PLD in the presence of inhibitors EDTA (1 mg/mL) and 1 mg/mL halopemide (purplish red solid line).

of reduced graphene oxide and fluorescein-labeled phospholipids was observed to only exhibit very weak fluorescence spectra with a peak intensity ∼227 at 514 nm. Compared with the fluorescence signal (a peak intensity ∼5222 at 514 nm) for FL-DHPE of the same concentration, the quenching efficiency for the fluorescein labels on the reduced graphene oxide surface was calculated to be 95.6%. After incubation of the nanoassembly with 1000 U/L phospholipase D, the reaction mixture showed a very strong fluorescence signal with a peak intensity ∼4370 at 514 nm and the fluorescence enhancement ratio was ∼19, evidencing the activation of fluorescence signals from these fluorescein labels during the reaction catalyzed by phospholipase D. Further control experiments were performed to verify that the fluorescence activation was specifically mediated by active phospholipase D. In the control where the nanoassembly was incubated with 1000 U/L phospholipase D in the presence of its inhibitor, halopemide (1 mg/mL), the fluorescence response gave a much smaller peak (intensity ∼624 at 516 nm) than that obtained with active phospholipase D. Because the only difference in these two reactions was the addition of the inhibitor, we inferred that inhibition of phospholipase D activity could specifically prevent the fluorescence activation. Furthermore, when we incubated the nanoassembly, 1000 U/L phospholipase D with two inhibitors, halopemide (1 mg/mL) and inhibitor EDTA (1 mg/mL), the resulting fluorescence spectrum showed little difference from that for the nanoassembly of reduced graphene oxide and fluorescein-labeled phospholipids. This revealed that the fluorescence activation was totally blocked by joint inhibition of phospholipase D activity, indicating the fluorescence activation was specific to phospholipase D activity. In addition, we performed the control experiment by adding high concentration of HSA in the nanoassembly solution. As anticipated, no appreciable fluorescence enhancement was observed in this case, which suggested the presence of abundant nonactive proteins cannot activate the fluorescence signal, thus confirming the specificity of the biosensor strategy. For a comparison of the phospholipid−graphene nanoassembly with its counterpart of graphene oxide in the assay of phospholipase D, we prepared the phospholipid-coated graphene oxide nanoassembly and examined its fluorescence responses. Surprisingly, the nanoassembly of graphene oxide and fluorescein-labeled phospholipids showed a relatively low fluorescence quenching efficiency and a small fluorescence peak was still observed at 514 nm with the intensity reading of ∼740. This was in good agreement with previous finding that the quenching efficiency of GO is significantly improved after reduction.[16] Such a low fluorescence quenching efficiency might be also attributed to the large areas of oxidized and hydrophilic spots on the graphene oxide surface which prevented phospholipids forming a compact assembly and increased the distance for fluorescence energy transfer. Moreover, after the phospholipase D-catalyzed reaction, the fluorescence signal displayed an appreciable activation, but the fluorescence enhancement ratio (∼2-fold) was much smaller than that obtained with the phospholipid−graphene nanoassembly. These findings indicated that improved activity of phospholipase D could be obtained for compactly assembled phospholipid substrates on nonoxidative graphene as compared with loosely assembled phospholipid substrates on graphene oxide, suggesting that the phospholipid−graphene nanoassembly provided an advantageous platform as a solubilized planar mimic of cellular membrane for phospholipid-related researches.

To verify whether the activated fluorescence was attributed to the release of the fluorescein labels, we performed fluorescence anisotropy and microcopy measurements. It was found that the fluorescence anisotropy profile displayed a remarkable increase after the phospholipase D-catalyzed reaction (Figure S8 in the Supporting Information), which suggested enzymatic reaction produced a fluorescent product with smaller size than the nanoassembly. This implied the fluorescein labels were cleaved and released from the nanoassembly. Microscopic analysis of the nanoassembly before and after the phospholipase D-catalyzed reaction further confirmed this finding (Figure S9 in the Supporting Information). Because of the presence of abundant fluorescein labels that were not completely fluorescently quenched on the surface, the nanoassembly was found to deliver a brighter fluorescence image on its surface before the enzymatic reaction than that obtained after the reaction. Therefore, these images confirmed the release of the fluorescein labels apart from the

dx.doi.org/10.1021/ac300539s | *Anal. Chem.* 2012, 84, 5944−5950

surface. In addition, we could exploit the unique capability of graphene as an efficient matrix for desorption/ionization of adsorbed molecules in surface-enhanced laser desorption/ionization time-of-flight mass spectrometry (SELDI-TOF MS) analysis.[5,31,38] This allowed us to directly validate the cleavage reaction catalyzed by phospholipase D (Figure S10 in the Supporting Information). Before the phospholipase D-catalyzed reaction, the nanoassembly gave a peak for DPPC (m/z: 735.2 and 756.5), while after the reaction, two peaks corresponding to the hydrolysis product phosphatidic acid (m/z: 687.2 and 725.2) appeared. These data gave immediate evidence for the cleavage reaction catalyzed by phospholipase D. It is noteworthy that this SELDI-TOF MS analysis also suggests the great potential of the developed phospholipid–graphene nanoassembly as a new platform for phospholipid-related research.

Performance of the Phospholipid–Graphene Nanoassembly-Based Biosensor for Phospholipase D. The ability of the nanoassembly-based biosensor for quantitative analysis of the activity of phospholipase D was then investigated. A series of samples containing phospholipase D of different concentrations were incubated with the nanoassembly at 37 °C for 2 h. Figure 4 displays typical fluorescence

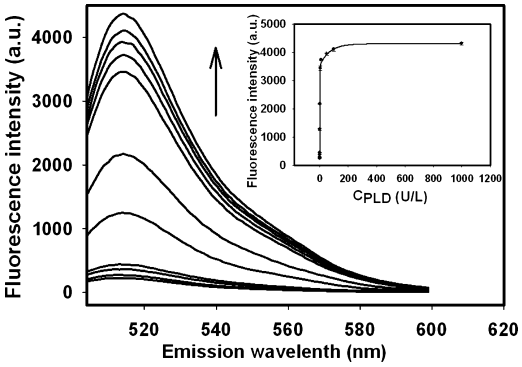

Figure 4. Fluorescence spectra obtained with PLD of varying concentrations (0, 0.025, 0.05, 0.1, 0.5, 1, 5, 10, 50, 100, 10^3 U/L). The arrow indicates the increase of PLD concentrations. Inset: plot of fluorescence intensities at 514 nm vs PLD concentrations. Error bars are standard deviation across four repetitive experiments.

spectral responses of the biosensor in these assays. As anticipated, the fluorescence spectra were observed to show dose-dependent activation in response to phospholipase D. The peak fluorescence readouts at 514 nm were dynamically increased (from ~273 to ~4370) with increasing concentrations of phospholipase D within the range of 0.025–1000 U/L. In terms of the rule of 3 times deviation over the blank response, the detection limit was estimated to be as low as 0.010 U/L (~4 pM). Such a low detection limit and a wide dynamic range of 5 orders of magnitude were much better (at least 1000-fold improvement) than existing strategies for phospholipase D assays.[29−32] Moreover, the biosensor showed very desirable reproducibility based on its homogeneous assay format. The relative standard deviations of peak fluorescence readouts were 3.0%, 2.5%, 0.8%, 0.7%, and 1.6%, respectively, in four repetitive assays of 0.025, 0.1, 1, 10, and 100 U/L of phospholipase D. These results implied that the developed biosensor provided a desirably sensitive and robust platform for activity assay of phospholipase D.

Further investigation of the biosensor for inhibition kinetics analysis was performed. We incubated phospholipid–graphene nanoassembly with 10 U/L PLD in the presence of inhibitor halopemide of varying concentrations (0, 10^{-6}, 10^{-5}, 10^{-4}, 10^{-3}, 10^{-2}, 0.1, 1 mg/mL) to obtain the inhibition curve (Figure S11 in the Supporting Information). Accordingly, the value of IC_{50} for halopemide could be calculated to be 5.76 μM for PLD.

The developed biosensor was also capable of monitoring in real time the hydrolysis catalyzed by phospholipase D, thereby offering kinetic information regarding the enzymatic reactions. To demonstrate this capability, we incubated the nanoassembly with different concentrations of phospholipase D and monitored the time-dependent fluorescence response profiles at 514 nm during the reactions, as shown in Figure 5.

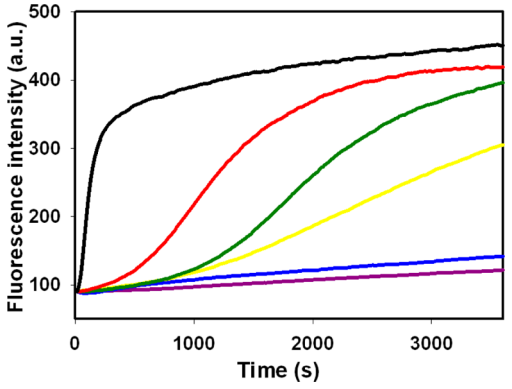

Figure 5. Time-dependent fluorescence response curves obtained for PLD of 0 (purple), 0.1 (blue), 1 (yellow), 10 (green), 100 (red), and 1000 U/L (black) at 25 °C.

Interestingly, after the addition of phospholipase D, we observed sigmoidal fluorescence activation profiles during the reactions, particularly in cases with medium concentrations of phospholipase D. In other word, the reaction rate was relatively slow at the initial period, became much faster at the middle period, and turned slower at the final period. A peculiar period in these reactions was the initial slow reaction rate phase, the so-called "lag phase".[39,40] This phase was originated from the weak binding affinity of phospholipases to the phospholipid substrates assembled on the nonoxidative graphene surface. During the lag period, the hydrolysis product phosphatidic acid was accumulated on the graphene surface into phosphatidic acid-rich microdomains. It was known that phosphatidic acid-rich microdomains could enhance binding affinity of phospholipases to the phospholipid monolayer and increase the local Ca^{2+} concentration to satisfy the requirement of phospholipases.[39,40] Thus, rapid hydrolysis was initiated and a sudden burst of fluorescence activation was obtained at the end of the lag phase. In addition, the duration of the lag phase, an important kinetic parameter for these reactions, was observed to be inversely proportional to concentration of phospholipase D. This indicated that the developed biosensor was able to offer insight into the kinetics of the hydrolysis reactions through real-time monitoring of the fluorescence activation responses.

■ CONCLUSIONS

A novel phospholipid–graphene nanoassembly was developed based on self-assembly of phospholipids on nonoxidative graphene surfaces. This nanoassembly could be prepared very easily through noncovalent hydrophobic interactions between

dx.doi.org/10.1021/ac300539s | Anal. Chem. 2012, 84, 5944–5950

the lipid tails and the graphene without destroying the electronic conjugation within the graphene sheet, ensuring the desired electrical and optical properties intrinsical in graphene. Moreover, the phospholipid coating afforded excellent biocompatibility, facile solubilization, and controlled surface modification for nonoxidative graphene, making the nanoassembly an advantageous and versatile platform over graphene oxide derivatives for biofunctionalization of graphene. It was revealed that the nanoassembly was composed of a bilayer of phospholipids with a graphene sheet hosting in the hydrophobic interior, creating a planar mimic of cellular membrane that might be potential for phospholipid-related researches. By using a fluorescein-labeled phospholipid in this nanoassembly, a novel fluorescence biosensor was then developed for activity assay of phospholipase D. The developed biosensor was demonstrated to have very high sensitivity because of improved efficiency of fluorescence energy transfer efficiency between the fluorophores and nonoxidized graphene. In addition, this biosensor offered excellent robustness, improved assay simplicity, and the capability for fluorescence-based real-time monitoring of the reaction kinetics.

■ ASSOCIATED CONTENT

Supporting Information

Description of other experimental procedures and additional figures. This material is available free of charge via the Internet at http://pubs.acs.org.

■ AUTHOR INFORMATION

Corresponding Author

*Phone: 86-731-88821961. Fax: 86-731-88821916. E-mail: tanglijuan@hnu.edu.cn (L.-J.T.); jianhuijiang@hnu.edu.cn (J.-H.J.).

Notes

The authors declare no competing financial interest.

■ ACKNOWLEDGMENTS

This work was supported by NSFC (21025521, 21035001, 21190041), the National Key Basic Research Program (2011CB911000), the CSIRT Program, and NSF of Hunan Province (10JJ7002).

■ REFERENCES

(1) Rümmeli, M. H.; Rocha, C. G.; Ortmann, F.; Ibrahim, I.; Sevincli, H.; Börrnert, F.; Kunstmann, J.; Bachmatiuk, A.; Pötschke, M.; Shiraishi, M.; Meyyappan, M.; Büchner, B.; Roche, S.; Cuniberti, G. *Adv. Mater.* **2011**, *23*, 4471−4490.
(2) Wang, Y.; Li, Z. H.; Wang, J.; Li, J. H.; Lin, Y. H. *Trends Biotechnol.* **2011**, *29*, 205−212.
(3) Liu, Z.; Robinson, J. T.; Sun, X. M.; Dai, H. J. *J. Am. Chem. Soc.* **2008**, *130*, 10876−10877.
(4) Gulbakan, B.; Yasun, E.; Shukoor, M. I.; Zhu, Z.; You, M. X.; Tan, X. H.; Sanchez, H. N.; Powell, D. H.; Dai, H. J.; Tan, W. H. *J. Am. Chem. Soc.* **2010**, *132*, 17408−17410.
(5) Wang, H. B.; Zhang, Q.; Chu, X.; Chen, T. T.; Ge, J.; Yu, R. Q. *Angew. Chem., Int. Ed.* **2011**, *50*, 7065−7069.
(6) Lu, C. H.; Yang, H. H.; Zhu, C.; Chen, L. X.; Chen, G. N. *Angew. Chem., Int. Ed.* **2009**, *121*, 4879−4881.
(7) Jang, H. J.; Kim, Y. K.; Kwon, H. M.; Yeo, W. S.; Kim, D. E.; Min, D. H. *Angew. Chem., Int. Ed.* **2010**, *49*, 5703−5707.
(8) Tang, L. H.; Wang, Y.; Liu, Y.; Li, J. H. *ACS Nano* **2011**, *5*, 3817−3822.
(9) Dong, H. F.; Gao, W. C.; Yan, F.; Ji, H. X.; Ju, H. X. *Anal. Chem.* **2010**, *82*, 5511−5517.
(10) Lin, L.; Liu, Y.; Zhao, X.; Li, J. H. *Anal. Chem.* **2011**, *83*, 8396−8402.
(11) Tang, L. A. L.; Wang, J.; Loh, K. P. *J. Am. Chem. Soc.* **2010**, *132*, 10976−11109.
(12) Cui, Y.; Kim, S. N.; Jones, S. E.; Wissler, L. L.; Naik, R. R.; McAlpine, M. C. *Nano Lett.* **2010**, *10*, 4559−4565.
(13) Artyukhin, A. B.; Shestakov, A.; Harper, J.; Bakajin, O.; Stroeve, P.; Noy, A. *J. Am. Chem. Soc.* **2005**, *127*, 7538−7542.
(14) Richard, C.; Balavoine, F.; Schultz, P.; Ebbesen, T. W.; Mioskowski, C. *Science* **2003**, *300*, 775−778.
(15) Nie, H. G.; Liu, S. J.; Yu, R. Q.; Jiang, J. H. *Angew. Chem., Int. Ed.* **2009**, *48*, 1−6.
(16) Loh, K. P.; Bao, Q. L.; Eda, G.; Chhowalla, M. *Nat. Chem.* **2010**, *2*, 1015−1024.
(17) Schultz, C. *Nat. Chem. Biol.* **2010**, *6*, 473−475.
(18) Hannun, Y. A.; Obeid, L. M. *Nat. Rev. Mol. Cell Biol.* **2008**, *9*, 139−150.
(19) Li, D.; Li, G. P.; Li, P. C.; Zhang, L. X.; Liu, Z. J.; Wang, J.; Wang, E. K. *Biomaterials* **2010**, *31*, 1850−1857.
(20) Song, J. B.; Cheng, L.; Liu, A. P.; Yin, J.; Kuang, M.; Duan, H. W. *J. Am. Chem. Soc.* **2011**, *133*, 10760−10763.
(21) Dubertret, B.; Skourides, P.; Norris, D. J.; Noireaux, V.; Brivanlou, A. H.; Libchaber, A. *Science* **2002**, *298*, 1759−1762.
(22) Al-Jamal, W. T.; Al-Jamal, K. T.; Cakebread, A.; Halket, J. M.; Kostarelos, K. *Bioconjugate Chem.* **2009**, *20*, 1696−1702.
(23) Gopalakrishnan, G.; Danelon, C.; Izewska, P.; Prummer, M.; Bolinger, P. Y.; Geissbuhler, I.; Demurtas, D.; Dubochet, J.; Vogel, H. *Angew. Chem., Int. Ed.* **2006**, *45*, 5478−5483.
(24) Eun, C. S.; Berkowitz, M. L. *J. Phys. Chem. A* **2011**, *115*, 6059−6067.
(25) Eun, C. S.; Berkowitz, M. L. *J. Phys. Chem. B* **2009**, *113*, 13222−13228.
(26) Ang, P. K.; Jaiswal, M.; Lim, C. H. Y. X.; Wang, Y.; Sankaran, J.; Li, A.; Lim, C. T.; Wohland, T.; Barbaros, O.; Loh, K. P. *ACS Nano* **2010**, *4*, 7387−7394.
(27) Athenstaedt, K.; Daum, G. *Eur. J. Biochem.* **1999**, *266*, 1−16.
(28) Hornberger, T. A.; Chu, W. K.; Mak, Y. W.; Hsiung, J. W.; Huang, S. A.; Chien, S. *Proc. Natl. Acad. Sci. U.S.A.* **2006**, *103*, 4741−4746.
(29) Fezza, F.; Gasperi, V.; Mazzei, C.; Maccarrone, M. *Anal. Biochem.* **2005**, *339*, 113−120.
(30) Ferguson, C. G.; Bigman, C. S.; Richardson, R. D; van Meeteren, L. A; Moolenaar, W. H.; Prestwich, G. D. *Org. Lett.* **2006**, *8*, 2023−2026.
(31) Lee, J.; Kim, Y. K.; Min, D. H. *J. Am. Chem. Soc.* **2010**, *132*, 14714−14717.
(32) Majd, S.; Yusko, E. C.; MacBriar, A. D.; Yang, J.; Mayer, M. *J. Am. Chem. Soc.* **2009**, *131*, 16119−16126.
(33) Ho, J. A. A.; Hsu, H. W. *Anal. Chem.* **2003**, *75*, 4330−4334.
(34) Hummers, W. S.; Offeman, R. E. *J. Am. Chem. Soc.* **1958**, *80*, 1339−1139.
(35) Park, S. J.; An, J. H.; Jung, I. H.; Piner, R. D.; An, S. J.; Li, X. S.; Velamakanni, A.; Ruoff, R. S. *Nano Lett.* **2009**, *9*, 1593−1597.
(36) Wei, Z. H.; Wang, D. B.; Kim, S.; Kim, S. Y.; Hu, Y. K.; Yakes, M. K.; Laracuente1, A. R.; Dai, Z. T.; Marder, S. R.; Berger, C.; King, W. P.; de Heer, W. A.; Sheehan, P. E.; Riedo, E. *Science* **2010**, *328*, 1373−1376.
(37) Stankovich, S.; Dikin1, D. A.; Dommett, G. H. B.; Kohlhaas, K. M.; Zimney, E. J.; Stach, E. A.; Piner, R. D.; Nguyen, S. T.; Ruoff, R. S. *Nature* **2006**, *442*, 282−286.
(38) Dong, X. L.; Cheng, J. S.; Li, J. H.; Wang, Y. S. *Anal. Chem.* **2010**, *82*, 6208−6214.
(39) Geng, D.; Chura, J.; Roberts, M. F. *J. Biol. Chem.* **1998**, *273*, 12195−12202.
(40) Estrela-Lopis, I.; Brezesinski, G.; Möhwald, H. *Biophys. J.* **2001**, *80*, 749−754.